Transport properties in manganite thin films

S. Mercone,[1] C. A. Perroni,[2] V. Cataudella,[2] C. Adamo,[1] M. Angeloni,[3] C. Aruta,[1] G. De Filippis,[2] F. Miletto,[2] A. Oropallo,[2] P. Perna,[4] A. Yu. Petrov,[1] U. Scotti di Uccio,[4] and L. Maritato[1]

[1]*Coherentia-INFM and Dipartimento di Fisica "E. R. Caianiello," Università di Salerno, Via S. Allende, 84081 Baronissi (SA), Italy*

[2]*Coherentia-INFM and Dipartimento di Scienze Fisiche, Università degli Studi di Napoli "Federico II," Via Cintia, 80126 Napoli, Italy*

[3]*Coherentia-INFM and Dipartimento di Ingegneria Meccanica, Universitá di Roma Tor Vergata, Via del Politecnico 1, 00133 Roma, Italy*

[4]*Coherentia-INFM and Di MSAT, Universita' di Cassino, Via Di Biasio 43, 03043 Cassino, Italy*

(Received 30 July 2004; revised manuscript received 28 October 2004; published 23 February 2005)

The resistivity of thin $La_{0.7}A_{0.3}MnO_3$ films (A=Ca, Sr) is investigated in a wide temperature range. The comparison of the resistivities is made among films grown by different techniques and on several substrates allowing to analyze samples with different amounts of disorder. In the low-temperature nearly half-metallic ferromagnetic state the prominent contribution to the resistivity scales as T^{α} with $\alpha \simeq 2.5$ for intermediate strengths of disorder supporting the theoretical proposal of single magnon scattering in presence of minority spin states localized by the disorder. For large values of disorder the low-temperature behavior of the resistivity is well described by the law T^3 characteristic of anomalous single magnon scattering processes, while in the regime of low disorder the α exponent tends to a value near 2. In the high temperature insulating paramagnetic phase the resistivity shows the activated behavior characteristic of polaronic carriers. Finally in the whole range of temperatures the experimental data are found to be consistent with a phase separation scenario also in films doped with strontium (A=Sr).

DOI: 10.1103/PhysRevB.71.064415 PACS number(s): 73.61.−r, 71.30.+h, 71.27.+a, 64.75.+g

I. INTRODUCTION

In the last years the mixed-valence perovskite manganese oxides $La_{1-x}A_xMnO_3$ (where A=Ca, Sr) have been intensively studied for their striking properties such as the colossal magnetoresistance (CMR).[1] The strong sensitivity to the magnetic field is found in the range $0.2 < x < 0.5$ at temperatures T around the ferromagnetic-paramagnetic (FP) transition point (the Curie temperature T_C) that is often close to the temperature T_p where a peak in the resistivity signals the metal-insulator (MI) transition.[2] The interplay between the Mn magnetic moments alignment and the metallic behavior is usually explained by invoking the double-exchange (DE) interaction,[3] that, however, only qualitatively accounts for the properties around the combined FP and MI transition.[4] As shown by many experimental results,[2,5,6] other interactions, mainly the coupling of the charge carriers with lattice, cooperate to drive the MI transition and the CMR effect. Actually a Jahn-Teller distortion of the oxygen octahedron can lead to the trapping of the charge carriers into a polaronic state influencing the transport properties in the high temperature phase. In these compounds the MI transition is affected by the crystal structure also because of the dependence of the Mn—Mn electron transfer matrix element on the Mn—O—Mn bond angle whose variation is a function of the radii of La^{3+} and A^{2+} cations.[7] Finally direct evidences of coexisting insulating localized and metallic delocalized components have been reported from many experimental techniques pointing out that the tendency toward phase separation is intrinsic in these compounds.[8] Indeed the phase coexistence arises from the complex interplay between electron, orbital, spin, and lattice degrees of freedom affecting most properties of the system near the phase boundary.

Even if a great effort has been done to understand the transport properties of these materials, a complete comprehension of the low temperature resistivity ρ in the half-metallic (HFM) ferromagnetic phase remains elusive. Indeed there is no agreement on the dependence of ρ as function of T in this phase. The law $\rho(T) - \rho_0 \sim T^2$, with ρ_0 residual resistivity, has been proposed to fit the data of single crystals in the low temperature range.[2,9–11] For the majority spin electrons the temperature dependence of the resistivity due to the electron-electron scattering would provide the T^2 dependence, however the T^2 term is about 60 times larger than the expected one for this type of scattering.[2] Another source for this T^2 behavior would be the single magnon scattering involving spin-flip processes,[12] but in a truly HFM system this process is suppressed since there is a band gap at the Fermi energy for one of the spin channels. On the other hand, the two-magnon scattering gives a $T^{9/2}$ dependence,[13] that is in disagreement with experimental data. Therefore in order to explain the behavior of ρ, it has been argued that in single crystals at intermediate temperatures the observed contribution could reflect the reappearance of minority spin states that become accessible to thermally excited magnons.[2,9] Of course this single magnon process becomes possible only if the spin polarization strongly decreases from unity with increasing T. In any case, in single crystals some experiments have found variations in the temperature scaling of ρ from T^2 to T^3 behavior, that is interpreted in terms of an anomalous single magnon scattering process.[14] This scattering channel opens at finite temperatures where the HFM structure of conduction can break down and, as a consequence, the rigid band approaches should not be justified. If one takes into account the nonrigid behavior due to spin fluctuations, the

 ©2005 The American Physical Society

inverse lifetime of the majority spin carriers is proportional to the density of state of the minority carrier band as well as the magnon density giving rise to the T^3 dependence in the low temperature resistivity.[15]

The situation in manganite films and ceramic samples is more complicated. Some researchers have interpreted the temperature behavior of the film resistivity as due to the T^2 term,[16,17] while others have attributed the low temperature dependence of ρ in $La_{1-x}Ca_xMnO_3$ and $La_{1-x}Sr_xMnO_3$ films to the polaron coherent motion.[18–20] Even if this latter process provides a good fit of the resitivity, the model requires the existence of exceedingly soft optical modes and polarons at almost zero temperature. In $La_{1-x}Ca_xMnO_3$ systems the electrical resistivity below T_C has been fitted also by a $T^{2.5}$ dependence.[21] This nonconventional result has been interpreted in these nearly HFM compounds taking into account a finite density of states of the minority spins at Fermi energy and their Anderson localization.[22] The spin-flip scattering involving single magnons can occur with finite probability giving a $T^{2.5}$ temperature dependence of the resistivity as result of the exact solution of the linear response equation. Therefore also in films and ceramics the transport properties at low T are considered to be strongly influenced by the single magnon scattering. Finally, in contrast to the behavior of single crystals, at high temperatures $La_{1-x}Sr_xMnO_3$ films are characterized by a decrease of the resistivity with increasing T signaling that an insulating phase becomes stable in the CMR region.[16]

Recently the attention has focused on the role of the disorder in these systems.[8] The effective strength of the intrisic disorder is influenced by several quantities, such as the tolerance factor since random potential fluctuations are due to different sizes and electronegativities of La^{3+} and A^{2+} cations. The random disorder is important to smear the first-order transition between competing states and to induce microscopic inhomogeneities.[23] Besides, random potential effects are able to give a large modification of the phase diagram near the bicritical point between charge-orbital ordering and FM states.[24] Actually the disorder suppresses the charge ordering, shifting the phase boundary between the ferromagnetic metal and the ordered insulator with respect to the case of the clean compound.[25] Even if the insulating phase is not directly triggered by the disorder in many compounds,[26] the effect of randomness controls the value of T_c and the transport properties at least at low temperature.[27] Actually measurements in $La_{1-x}Sr_xMnO_3$ single crystals and polycrystalline compounds,[28,29] and $La_{1-x}Ca_xMnO_3$ films[30,31] have shown that the low temperature resistivity exhibits a shallow minimum. There is a quite general consensus upon the influence of electron-electron interaction with scattering from static inhomogeneities as the dominant mechanisms for the upturn. However it is not clear what is the role of the disorder on the electrical resitivity for temperatures larger than that of the minimum but smaller than T_p.

In this paper, we report on our measurements of resistivity in $La_{0.7}Sr_{0.3}MnO_3$ (LSMO) and $La_{0.7}Ca_{0.3}MnO_3$ (LCMO) films grown by different techniques and on several substrates. The availability of samples prepared in different ways is of great advantage in this context for several reasons. First of all, it is easier to address possible systematic errors due to sample-dependent effects. In fact, the resistivity may be determined not only by intrinsic mechanisms, but also by other contributions such as grain boundaries, local defects and spurious phases. Second, it is possible to study samples that differ for strain and thickness, and that show different values of T_p and of resistivity. Since the residual resistivity is a measure of the global disorder, this implies the possibility to investigate the role of disorder in the transport properties of manganites. Finally, the analysis has dealt with two classes of manganite compounds (LSMO and LCMO) since they are characterized by different properties in the CMR range. Indeed LSMO systems show the highest critical temperatures, weak-to-intermediate electron-phonon (el-ph) coupling and disorder, whereas LCMO systems demonstrate MI transition at lower temperatures and belong to the group of manganites with intermediate-to-strong el-ph and disorder strength.[8,32]

In Sec. II of this paper we briefly describe the different experimental techniques used for growing and characterizing films. In Sec. III we report the obtained results along with the theory which supports them. Indeed in Sec. III A we carry out a detailed study of the charge transport at low temperature ($T<T_p$). In the region of the ferromagnetic metallic (FM) state the temperature contribution scales as T^α with α close to 2.5 for an intermediate range of residual resistivities supporting the role of single magnon scattering when, due to the disorder, the minority spin states are localized.[22] For large values of disorder the resistivity scales with the law T^3 characteristic of anomalous single magnon scattering processes, while in the regime of low disorder α tends to a value near 2. These behaviors are quite robust since they are independent of the film size and the strain distribution. In Sec. III B the high temperature ($T>T_p$) resistivities are discussed showing that the activated behavior characteristic of polaronic carriers is present in the films. Finally in the whole range of temperature the experimental data are consistent with a phase separation scenario also in LSMO films.

II. EXPERIMENT

We considered LSMO and LCMO films prepared by the following different techniques: (a) pulsed laser deposition (PLD); (b) molecular beam epitaxy (MBE); (c) sputtering. We briefly summarize the fabrication technique of the samples.

A. PLD

The PLD deposition was carried out by using a KrF excimer laser ($\lambda = 248$ nm) with a repetition rate of 3 Hz. The pulse width was 25 ns, and pulse energy 150 mJ. The substrates have been held at 700 °C in oxygen atmosphere ($P_{O_2} = 50$ Pa) 50 mm far from the target. After film growth, the samples were cooled at room temperature in about 10 minutes in oxygen at 0.5 bar. Two different samples have been considered in this work. The first one is a 300 nm LCMO, the second a 160 nm thick LSMO. The first sample has been deposited onto on a (100) $SrTiO_3$ (STO) substrate, while the second on (100) $LaAlO_3$ (LAO). X-ray diffraction

TABLE I. Representative samples obtained by different fabrication techniques. For the films with (110) orientation we have reported the values of the lattice parameters in the text.

Technique	Name	Composition	Sustrate (h,k,l)	Thickness (Å)	T_p (K)	c axis (Å)	Rocking width
PLD	PCS0	$La_{0.7}Ca_{0.3}MnO_3$	$SrTiO_3(100)$	3000	(245 ± 1)	3.86 ± 0.01	0.2 deg
PLD	PSL0	$La_{0.7}Sr_{0.3}MnO_3$	$LaAlO_3(100)$	1600	(364 ± 2)	3.87 ± 0.01	0.2 deg
MBE	MSS0	$La_{0.7}Sr_{0.3}MnO_3$	$SrTiO_3(100)$	350	(344.6 ± 0.1)	3.79 ± 0.01	0.1 deg
MBE	MSN1	$La_{0.7}Sr_{0.3}MnO_3$	$NdGaO_3(110)$	210	(>400)	3.9 ± 0.1	0.1 deg
Sputtering	SSS1	$La_{0.7}Sr_{0.3}MnO_3$	$SrTiO_3(110)$	400	(400 ± 1)		<0.1 deg
Sputtering	SSS0	$La_{0.7}Sr_{0.3}MnO_3$	$SrTiO_3(100)$	400	(350 ± 1)	3.85 ± 0.01	<0.1 deg
Sputtering	SSL1	$La_{0.7}Sr_{0.3}MnO_3$	$LaAlO_3(110)$	400	(380 ± 1)		<0.1 deg

(XRD) measurements in the Bragg-Brentano configuration yield a lattice spacing close to that of LCMO and LSMO bulks, respectively. Considering the relatively high thickness value, it is reasonable to assume that the stress due to the substrate is completely relaxed in these samples.[33]

B. MBE

Thin LSMO samples on different substrates have been deposited by MBE in the same batch, using a codeposition procedure in which the elemental rates of La (*e*-beam source), Sr and Mn (effusive cells) have been carefully controlled to obtain the desired sample composition. The (100) STO, (110) $NdGaO_3$ (NGO), and (100) LAO substrates have been held at 700 °C during growth. The peculiarity of the MBE is the possibility to achieve the in-situ formation of the perovskitic phase at very low oxygen pressure without any post-annealing treatment. In this case, a mixture of O_2 +5% ozone at a total pressure $P=2.6\times10^{-2}$ Pa was employed. The atmosphere composition inside the deposition chamber has been controlled by mass spectroscopy. The reflected high energy electron diffraction (RHEED) analysis has been performed during the growth process to check the structural properties of the films. Through reflectivity measurements we have studied the surface roughness and the thickness of the thin films. Details of these surface analysis, EDS, and x-ray diffraction are reported elsewhere.[34]

C. Sputtering

Several LSMO samples have been deposited by on axis RF magnetron sputtering on various substrates, i.e., on (100) and (110) STO, and on (110) LAO. The deposition conditions that give the best samples in terms of cation stoichiometry, crystal structure, and transport properties are the following. The sputtering pressure (50% O_2, 50% Ar mixture) has been varied in the range 50–70 Pa. The substrates have been held at 840 °C 40 mm far from the LSMO target. Such samples are smooth, highly ordered, and as a general rule present low resistivity and high Curie temperature. Moreover, some films have also been deposited in non optimized conditions, yielding samples with reduced T_p and higher resistivity. More details on the fabrication procedure and a careful structural characterization of samples with both (100) and (110) orientation are discussed in a separate paper.[35] Briefly, the films deposited on both (100) and (110) substrates grow in the usual cube-on-cube mode. The samples deposited on (110) STO (SSS1 in Table I) are fully strained with lattice parameters $a=3.89\pm0.01$ Å, $b=3.89\pm0.01$ Å, and $c=3.91\pm0.01$ Å. The sample grown on (110) LAO is instead completely relaxed with lattice parameters $a=b=c=3.89\pm0.01$ Å.

XRD analysis in the Bragg-Brentano configuration has been performed on the produced samples after deposition in order to characterize their crystal properties. For each technique a very careful investigation of epitaxy, orientation, strain, crystal quality, and twinning was performed by using different kinds of analysis. All the samples that have been analyzed in this work show high structural quality. This has been assessed by the observation of sharp rocking curves and of the interference fringes around the reflections in $\theta-2\theta$ scans. Typical values of the rocking curve width are shown in Table I. The stoichiometry of these samples has been determined by energy dispersive spectroscopy (EDS) for samples deposited on MgO with the same deposition parameters. Recently we have also carried out atomic force microscopy measurements which confirm the low roughness and the good quality of the samples. Some structural parameters of the representative samples[33–35] are summarized in Table I. As reported in this table, there is a large variety in the film thickness, strain and substrate orientation of the films. All the characterizations allow us to confirm the homogeneity of their growth and to affirm that the film are epitaxial.

The measurement of the temperature dependence of resistivity in zero magnetic field was performed in the standard four-probe configuration, with the usual compensation of thermoelectric bias by inversion of the direction of current flow. Electrical contacts to the samples are provided by direct indium soldering on the manganite film, or by soldering on Au pads deposited by sputtering. In both cases, the contact area is ~1 mm^2. The van der Pauw technique is employed to deduce the geometrical factor that allows estimation of resistivity.[36] To this aim, thickness values are provided by calibration to the oscillations of the x-ray reflectivity. We checked the error introduced by the geometrical configuration of the contacts by repeated evaluations after removal and replacement of the contacts. Also taking into account the experimental error in the measurement of samples thickness, we estimate that the error in the geometrical factor is about 10%. Part of the measurements have been performed resort-

ing to a cryogenic inset in a He bath; in others a cryocooler was employed. In both cases, we devoted a special care to the problem of sample thermalization and temperature measurement. On the experimental basis, both the measurement techniques lead to small spurious thermal hysteresis in a cooling-heating cycle of measurement. The effect on the determination of the physical parameters in the fitting session is negligible, as discussed in the following.

III. RESULTS AND DISCUSSION

The resistivity curves present general features. Indeed all the samples are characterized by the MI transition marked by the temperature T_p. As shown in Table I, there is a large variation in the values of T_p according to the growth technique, the thickness and the strain. Besides, below 20 K the resistivity of our samples shows a shallow upturn that has been interpreted as due to quantum interference effects in presence of disorder.[28–31] Since this issue is beyond the purpose of the present work, we have focused on the temperature dependence of the resistivity starting from the minimum.

In the following sections the low and the high temperature regimes of the resistivities will be studied in detail.

A. Low temperature range

The $\rho(T)$ plots of all the samples have been fitted by the following function:

$$\rho(T) = \rho_0 + AT^{\alpha}, \tag{1}$$

with ρ_0, A, and α free parameters. Here ρ_0 is the residual resistivity that we consider as a measure of the effective disorder, and AT^{α} a generic T-power law which can simulate different scattering processes. Typical values of the residual resistivity ρ_0 are always less than 4×10^{-3} Ω cm which can be considered a check of high quality of the samples. Together with the results obtained on the behavior of the $\rho(T)$ shown in the following, this feature represents an important argument which supports the absence of any kind of effect on the resistivity rising from grain diffusion. As observed by Gupta *et al.*,[37] even grains of the order of 10 μm have strong effects on both ρ_0 and $\rho(T)$ at low temperatures. In fact, due to the diffusion by grain surface, the ρ_0 becomes higher and the behavior of ρ changes as a function of temperature. As it will be shown in the following results, this is not the case for our resistivity data. Thus we can conclude that grain boundary effect can be neglected in our analysis.

In Fig. 1 we plot the resistivity measurements and the corresponding fits of two representative samples (a PSS0 and a MSS0) in three different ranges of temperature, 4–60 K, 4–120 K, and 4–200 K. In Table II we report the parameters ρ_0, A, and α defined in Eq. (1) for the different fit sessions, together with the coefficient of determination R^2. In any range of temperature, the fit provides an excellent approximation of the experimental data (R^2 very close to 1). The sensitivity of the fit to the value of the parameter α has been checked in the following way. Once the best fit parameters are determined, α is fixed at value different from the optimal estimate, and ρ_0 and A are calculated by a new fit registering

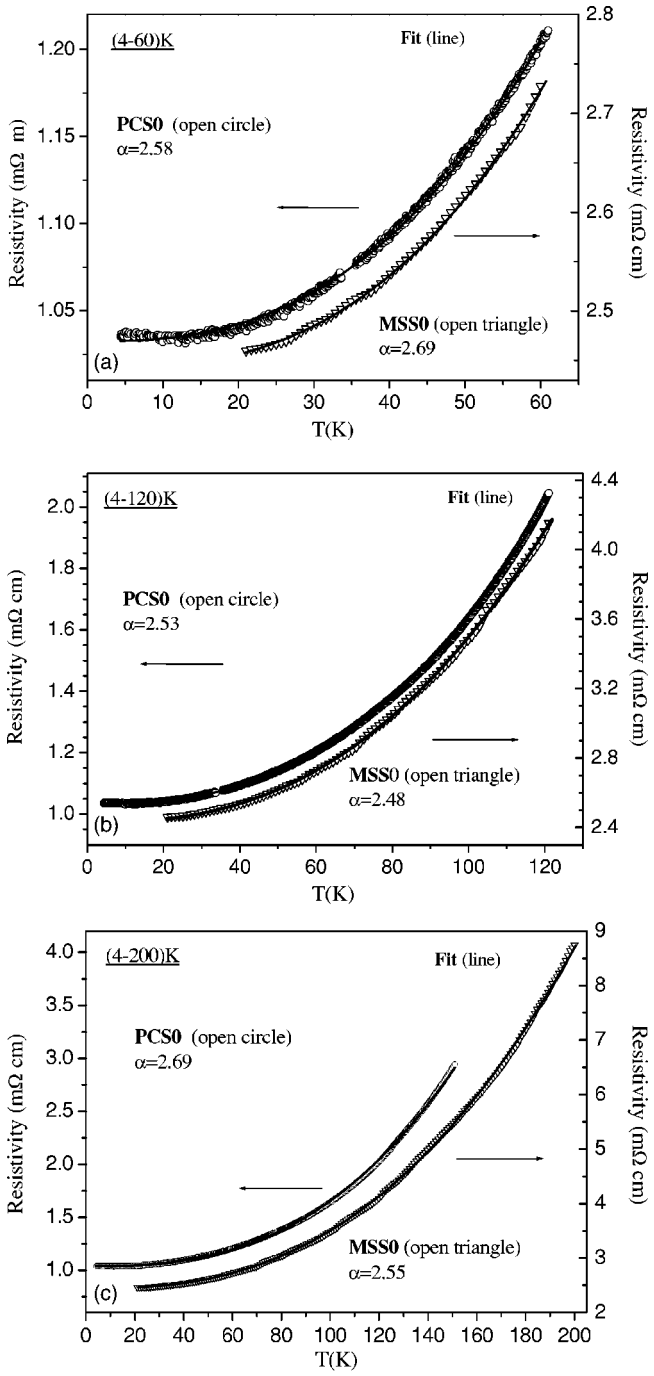

FIG. 1. Low-temperature resistivity in three different ranges, (a) range between 4 K and 60 K, (b) range between 10 K and 120 K, and (c) range between 10 K and 200 K. Experimental data of PSS0 (open circle) and MSS0 (open triangle) films are shown with the corresponding fits (line).

the variation of R^2. As a rule, a variation $\Delta\alpha=0.1$ leads to ΔR^2 larger than 10^{-4}. The comparison of the data in Table II also suggests the following considerations on the reliability of the values of the fit parameters. First of all, it is seen that ρ_0 is not affected by the choice of the fitting interval. The statistical error on ρ_0 is negligible, therefore the overall error is due to the experimental uncertainty on the geometrical factor, as discussed in the preceding section. The case of α is

TABLE II. Samples obtained from different growth techniques analyzed in a wide range of temperatures.

Sample	Range T (K)	ρ_0 (Ω cm)	**A** (Ω cm K$^{-\alpha}$)	α	R^2
PCS0	4–60	0.00103	4.33×10^{-9}	2.58	0.99892
PCS0	4–120	0.00103	5.31×10^{-9}	2.53	0.99970
PCS0	4–150	0.00104	2.49×10^{-9}	2.69	0.99960
MSS0	20–60	0.00244	4.47×10^{-9}	2.69	0.99905
MSS0	20–120	0.00243	1.16×10^{-8}	2.48	0.99953
MSS0	20–200	0.00244	8.38×10^{-9}	2.55	0.99973

different, because a variation is typically observed when different ranges of temperature are considered. Also the choice of the lower limit of the temperature range deserves attention, because of the shallow upturn of resistivity at low temperature. This region has been excluded from the range of the fit by Eq. (1), because they are out of the limits of validity of the model. Our analysis of the data leads to the conclusion that an overall uncertainty $\Delta\alpha=\pm0.1$ results from the different possible choices of the temperature range. In view of the physical interpretation of this parameter in the overall temperature range, we argue that this is the uncertainty of the whole procedure (measurement and fit session). Other experimental and statistical effects are in fact negligible. As an instance, we checked that the error due to the thermal coupling of the samples (i.e., the finite value of dT/dt during the measurements, with consequent shift of temperature between sample and thermometer) is well below 0.1 in all measurements.

In previous investigations the deviation from the quadratic power law has been ascribed to a combination of terms due to different kinds of scattering.[17,18,20] In order to understand if this analysis can be performed also for our samples, we have carried out the fits of the data with some possible combinations of terms. So we have used the following equation to fit the data:

$$\rho(T) = \rho_0 + AT^2 + S, \tag{2}$$

where S stands for the term due to the scattering with anomalous single magnons[14] (T^3), two magnons[13] ($T^{9/2}$), spin-waves[20] ($T^{7/2}$), acoustic phonons[17] (T^5), and optical phonons (proportional to the phonon thermal distribution with the frequency ω_0 fit parameter). Even giving a larger weight to the data at very low temperature, we did not succeed in obtaining the excellent agreement that we obtained with Eq. (1) (it always provides the fit coefficient R^2 closes to 1). This result points out that the $T^{2.5}$ dependence in our samples cannot be simulated through a combination of different power laws, as assumed previously.[21] Moreover this behavior finds a natural explanation within a theory that considers the role of the disorder in nearly HFM systems.[22] By taking into account a finite density of states of the minority spins at Fermi energy and the Anderson localization of them, the spin-flip scattering involving single magnons can occur with finite probability. Resolving the linear response equation, the temperature dependence of the resistivity is given by $T^{2.5}$ starting from a low characteristic temperature.

The analysis described above has been performed for all the 23 samples obtained changing the film sizes, strains, compounds (LSMO and LCMO) measuring ρ in films fabricated with several techniques or in films grown by the same technique with different deposition parameters. In order to compare the different results, we have chosen the same fitting temperature range (20–100) K. Actually this temperature range is far enough from the MI transition temperature in order to avoid any spurious effect due to vicinity of the MI transition. At the same time, the 20 K lower bound is quite large in order to avoid the effects in temperature dependence of ρ due to the upturn at low T. In Fig. 2 we show the typical resistivity curves and relative fitting values of some of the samples. There is evidence of a correlation between the residual resistivity and fitting parameter α. Therefore the values of α versus ρ_0 are reported in Fig. 3 for all the analyzed films. Quite surprisingly most films present a value of α very close to 2.5. In particular all the samples in the range $0.04\ \text{m}\Omega\ \text{cm}<\rho_0<1\ \text{m}\Omega\ \text{cm}$ have a value equal to 2.5 within the estimated error bar. Our data show a deviation from $T^{2.5}$ dependence for both high and low ρ_0. In particular for $1\ \text{m}\Omega\ \text{cm}<\rho_0<10\ \text{m}\Omega\ \text{cm}$ the α exponent approaches the value 3. Finally for $\rho_0\leqslant0.4\ \text{m}\Omega\ \text{cm}$ we find evidence of a tendency towards small α values.

We notice that in the set of fabricated samples ρ_0 varies from 0.03 mΩ cm, that represents one of the lowest values in manganites, to 6 mΩ cm. Therefore all the samples are char-

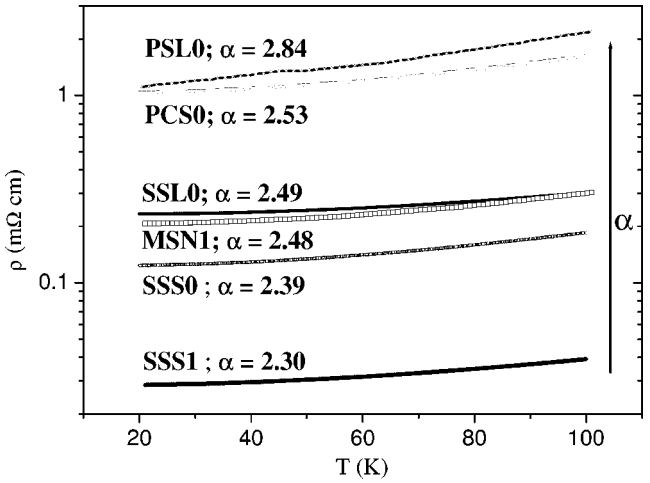

FIG. 2. Low-temperature resistivities with corresponding fits in the range between 20 K and 100 K for different films. The fits are obtained by Eq. (1) where the fit exponent α is defined.

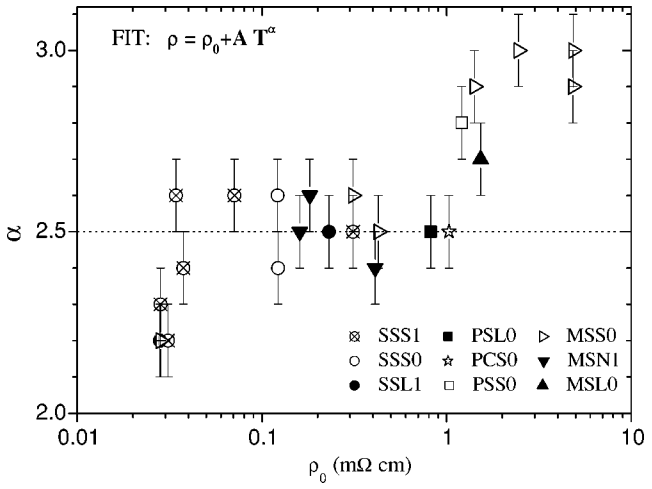

FIG. 3. Low-temperature fit exponent α as a function of the residual resistivity ρ_0.

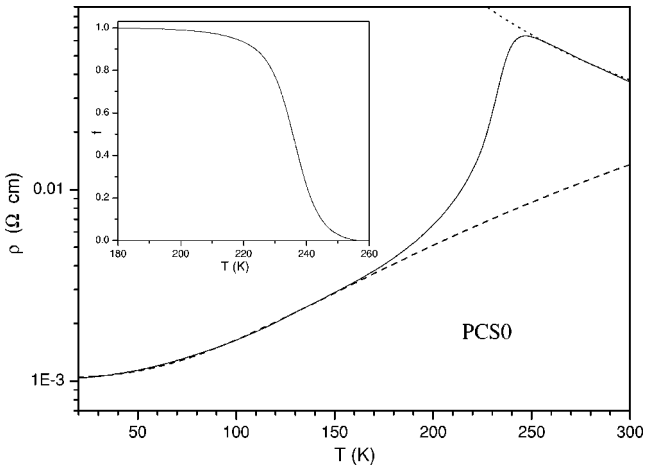

FIG. 4. Resistivity of the PCS0 film (solid line) as a function of the temperature. The dotted line stands for the low-temperature fit, while the dashed line for the high-temperature one. In the inset the distribution function f derived through Eq. (4) is reported.

acterized by a residual resistivity ρ_0 smaller than the Mott's maximum metallic resistivity that is of the order of $\simeq 10$ mΩ cm in these systems.[27] Moreover most films are characterized by $\rho_0 < \rho_c \simeq 1$ mΩ cm, a critical value that has been suggested to be a lower bound for the occurrence of an Anderson MI transition with increasing the temperature.[38] As discussed above, for moderate disorder (0.04 mΩ cm$< \rho_0 < \rho_c$), the single-magnon scattering assisted by the localized minority spin states explains the transport properties in the low-T range. However starting just from ρ_c a new scattering mechanism sets in. The value $\alpha = 3$ has been previously interpreted as due to an anomalous single magnon scattering that can become dominant with the decrease of spin-wave stiffness coefficient, that is proportional to the one-electron bandwidth of the e_g carriers.[14,15] With increasing the strength of the disorder, it is possible that the effective bandwidth of the itinerant charge carriers gets reduced. Therefore this new transport regime is consistent with the increased strength of disorder and is in agreement with previous experimental investigations made on Nd-doped manganite systems with large values of ρ_0.[39] Finally in the regime of small disorder ($\rho_0 \simeq 0.03-0.04$ mΩ cm) the α exponent tends toward the value 2 that is characteristic of single crystals.

In the next section we will analyze the transport properties at high temperature pointing out the strong interplay between disorder and el-ph coupling in determining the insulating phase. In fact it has been stressed that effects due to disorder should not be able alone to drive the MI transition.[26] However, it has been also shown that effects due to disorder can enhance the tendency toward the polaron formation and the sensitivity to changes in the el-ph coupling.[40]

B. Whole temperature range

In this section we analyze the resistivity in the high and the whole T range.

Single crystals and optimized films of LCMO show the MI transition at close temperatures. Even if the strength of the intrinsic disorder in these materials is not negligible, the transport properties in the PI phase are typically described in terms of polaronic conduction stressing the role of the el-ph interaction in driving the MI transition.[2] For $T > T_p$ the resistivity is characterized by an activated behavior that can be described by the following law:

$$\rho_{\mathrm{PI}}(T) = \rho_\infty \cdot \exp\left(\frac{E_g}{K_B T}\right), \tag{3}$$

with the activation energy E_g of the order of 0.1–0.2 eV. In particular, in the insulating phase, a high temperature expansion of the polaronic resistivity gives the dependence $\rho_\infty \propto \sqrt{T}$ and $E_g = E_p/2$, with E_p polaron binding energy.[41] In the PCS0 sample the best fit to ρ is provided by the polaronic hopping mechanism. Other forms such as those predicted by variable range hopping[42] were also used to fit the data, but they yield less accurate fits (R^2 remarkably smaller than unity). In Fig. 4 the plot of the resistivity is reported in the temperature range up to 300 K. For the LCMO film the best fit is obtained for $E_g = 82.15$ meV that is consistent with the results of previous investigations. Clearly in this regime the role of the correlation between polarons can be important since it gives rise to charge ordering fluctuation.[43]

In order to interpret the transport properties in the intermediate range of T, the effects of the phase separation between FM and PI phases have been invoked.[2,17,32] If the properties of these systems are driven by the coexistence of FM and PI phases,[41] $\rho(T)$ can be written as

$$\rho(T) = \rho_{\mathrm{FM}} \cdot f + \rho_{\mathrm{PI}} \cdot (1 - f), \tag{4}$$

where ρ_{FM} is given by Eq. (1) and ρ_{PI} by the polaron hopping term of Eq. (3). The function f represents the volume fraction of the FM metallic regions in the system while $(1-f)$ represents the paramagnetic one. This function has a value equal to unity at low temperatures, is decreasing with increasing T and goes to zero in the PI phase. The fits of the data in the low and high temperature region, given by Eqs. (1) and (3), respectively, are extended in the whole tempera-

ture range, so we have extracted the distribution function f using for $\rho(T)$ in Eq. (4) the experimental data. The function f reported in the inset of Fig. 4 is in qualitative agreement with the fraction of volume calculated within a single-orbital model that takes into account the combined effect of the magnetic and el-ph interactions.[41] Actually, in agreement with many other theoretical works and experimental observations,[8] the combined effect of these interactions pushes the system toward a regime of two coexisting phases: one made by itinerant carriers forming ferromagnetic domains and another by localized polarons giving rise to paramagnetic or antiferromagnetic domains depending on temperature.

The analysis of the transport properties in the whole temperature range is challenging for LSMO systems. In fact, single crystals of LSMO are metallic ($d\rho/dT>0$) in any range of temperature. However, even when the conduction is metallic, a high temperature polaronic behavior is directly observed by means of photoemission, x-ray absorption and emission, and extended x-ray absorption fine structure spectroscopy.[44,45] Moreover, unlike single crystals, in LSMO films the FP transition is accompanied by a close MI transition, as in LCMO systems. The role played by both el-ph coupling and disorder can be crucial in stabilizing the insulating phase. Actually it has been shown that there is a positive feedback of disorder on the polaron formation and an increase of the sensitivity of the system to variations of el-ph coupling.[46] In a regime of moderate disorder, at high temperatures the system can change from a metallic ($d\rho/dT>0$) to an insulating ($d\rho/dT<0$) behavior by means of a slight increase of the el-ph coupling. Therefore in the films, where effects of disorder can be stronger and the strain is able to increase the el-ph coupling,[20,32] the interplay of disorder and el-ph coupling can be able to drive a MI transition absent in the single crystal bulk case.

The LSMO films grown by different techniques and analyzed in this work show MI transition temperatures ranging from 300 K to values slightly larger than 400 K. We find that the value of T_p generally increases as the residual resistivity decreases even if this MI transition temperature is strongly dependent also by other factors such as the film thickness, the orientation, and the value of the strain. Therefore it not easy to recognize a clear relation between T_p and ρ_0 unless the other parameters are under strict control. In Fig. 5 we show the results obtained on two different doped samples, SSS0 grown on (100) STO and SSS1 on (110) STO. These two samples have residual resistivities smaller than $\rho_c \simeq 1$ mΩ cm, therefore at low temperature the temperature dependence of ρ is dominated by the $T^{2.5}$ contribution. At high T both SSS0 and SSS1 resistivities show an activated behavior, so the best two-parameter fit is given by Eq. (3). Moreover we have found that the parameters considered in variable range hopping mechanism, such as the localization length, show variations of many orders of magnitude for films with close values of residual resistivity and critical temperature (for example, data shown in Fig. 5). The sample SSS1 shows a sharp maximum in the resistivity that in the range 500–800 K is well described by Eq. (3) with $\rho_\infty \propto \sqrt{T}$ and an activated energy E_g equal to 64.37 meV. Instead the

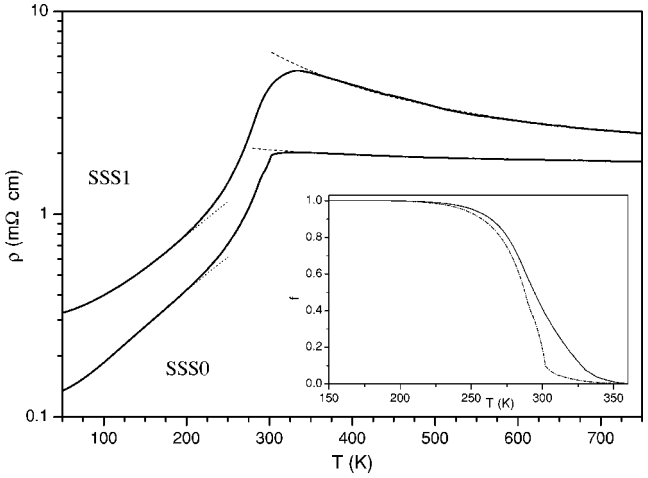

FIG. 5. Resistivities of the SSS0 and SSS1 as a function of the temperature. The dotted lines stand for the low-temperature fits, while the dashed line for the high-temperature ones. In the inset the distribution functions f derived through Eq. (4) for SSS0 (dotted-dashed line) and SSS1 (solid line) films are plotted.

sample SSS0 is on the verge of the metallic phase, in fact the resistivity is weakly decreasing and the activation energy is an order of magnitude smaller than that of SSS1. Therefore the different behavior of the resistivities of two samples correlates with the decrease of the residual resistivity. Indeed for LSMO films with ρ_0 smaller than 0.1 mΩ cm and T_p larger than 400 K the resistivity is characterized by a broad maximum around T_p and it decreases very slowly as a function of the temperature in the insulating side. Finally, on the basis of recent investigations reporting phase separation also in LSMO films,[45,47] we propose to interpret the resistivity data on the whole temperature range employing Eq. (4). Following the same procedure used for LCMO films, we can extract the distribution function f that provides the volume fraction of the FM phase in the system. The distribution functions for the two samples (inset of Fig. 5) bear a strong resemblance with those obtained in the case of the LCMO films, in fact there is only a slower variation in temperature. Hence these data seem to confirm that the phase separation scenario can adopted also in the analysis of the transport properties of LSMO films.

Comparing Fig. 4 and Fig. 5, there is also a correlation between the residual resistivity and the activation energy. By increasing ρ_0, the samples are characterized by a larger activation energy that is a measure of the coupling of the charge carriers to the lattice. Therefore these data confirm the interplay of disorder and el-ph coupling that represent key parameters in order to understand the properties of these materials and in particular the CMR effect.[8,24,25,48]

IV. SUMMARY

In this paper we have discussed the transport properties of LCMO and LSMO films for temperatures up to 800 K. We have made the comparison of the results between films grown by different techniques since this gives the possibility to investigate samples with different amounts of disorder re-

maining in the FM phase. The first part of our analysis has focused on the low temperature range where we have found clear evidence that the temperature contribution scales as T^{α} with α close to 2.5 for an intermediate range of residual resistivities. For large values of disorder the temperature dependence of the resistivity fits well the law T^3 characteristic of anomalous single magnon scattering processes, while in the regime of low strength of disorder α shows a tendency towards a value near 2. These results are independent of the film thickness, on the strain distribution and on the growth technique, and supports the role of the single magnon scattering. At high temperatures the activated behavior of polaronic carriers represents the prominent behavior in most films where the disorder seems to increase the tendency toward the polaron formation and correlates with the activation energy. In the whole range of temperatures the experimental data seem to support a phase separation scenario that has been proposed by recent studies also in LSMO systems.

In order to further elucidate the low T behavior of resistivity, it would be interesting to pursue the study of the transport properties in presence of magnetic field. When an external field is applied, the disorder is expected to be reduced influencing not only the upturn around 10–20 K (Refs. 30 and 31) but also the single magnon scattering.[22] The analysis in magnetic field will be the subject of a future study.

ACKNOWLEDGMENTS

This work has been partially supported by PRIN project "strain effects on the metal-insulator transition and on the metallic state of manganite thin films and heterostructures" of the Italian Minister of the University and Research (MIUR). Three of the authors (S.M., C.A., and A.O.) are supported by "Regione Campania" within the project "Creazione di operatori per il trasferimento tecnologico da enti pubblici di ricerca a piccole e medie imprese" managed by CRdC (Centro Regionale di Competenza) of Universita di Napoli "Federico II." Two of the authors (P.P. and U.S.) acknowledge partial support by the MIUR under the PRIN project "sviluppo di materiali avanzati e nuove tecnologie di produzione per applicazioni nel campo della sensoristica."

[1] R. von Helmolt, J. Wecker, B. Holzapfel, L. Schultz, and K. Samwer, Phys. Rev. Lett. **71**, 2331 (1993); S. Jin, T. H. Tiefel, M. McCormack, R. A. Fastnacht, R. Ramesh, and L. H. Chen, Science **264**, 413 (1994).
[2] M. B. Salamon and M. Jaime, Rev. Mod. Phys. **73**, 583 (2001).
[3] C. Zener, Phys. Rev. **81**, 440 (1951); **82**, 403 (1955).
[4] A. J. Millis, P. B. Littlewood, and B. I. Shraiman, Phys. Rev. Lett. **74**, 5144 (1995); A. J. Millis, B. I. Shraiman, and R. Mueller, *ibid.* **77**, 175 (1996).
[5] M. R. Ibarra, P. A. Algabarel, C. Marquina, J. Blasco, and J. Garcia, Phys. Rev. Lett. **75**, 3541 (1995).
[6] A. J. Millis, Nature (London) **392**, 147 (1998).
[7] H. Y. Hwang, S.-W. Cheong, P. G. Radaelli, M. Marezio, and B. Batlogg, Phys. Rev. Lett. **75**, 914 (1995).
[8] E. Dagotto, *Nanoscale Phase Separation and Colossal Magnetoresistance* (Springer-Verlag, Heidelberg, 2003).
[9] M. Jaime, P. Lin, M. B. Salamon, and P. D. Han, Phys. Rev. B **58**, R5901 (1998).
[10] A. Urushibara, Y. Moritomo, T. Arima, A. Asamitsu, G. Kido, and Y. Tokura, Phys. Rev. B **51**, 14 103 (1995).
[11] T. Okuda, A. Asamitsu, Y. Tomioka, T. Kimura, Y. Taguchi, and Y. Tokura, Phys. Rev. Lett. **81**, 3203 (1998); T. Okuda, Y. Tomioka, A. Asamitsu, and Y. Tokura, Phys. Rev. B **61**, 8009 (2000).
[12] I. Mannari, Prog. Theor. Phys. **22**, 335 (1959).
[13] K. Kubo and N. Ohata, J. Phys. Soc. Jpn. **33**, 21 (1972).
[14] T. Akimoto, Y. Moritomo, A. Nakamura, and N. Furukawa, Phys. Rev. Lett. **85**, 3914 (2000).
[15] N. Furukawa, J. Phys. Soc. Jpn. **69**, 1954 (2000).
[16] G. J. Snyder, R. Hiskes, S. DiCarolis, M. R. Beasley, and T. H. Geballe, Phys. Rev. B **53**, 14 434 (1996).
[17] G. Li, H.-D. Zhou, S. J. Feng, X.-J. Fan, and X.-G. Li, J. Appl. Phys. **92**, 1406 (2002).
[18] G.-M. Zhao, V. Smolyaninova, W. Prellier, and H. Keller, Phys. Rev. Lett. **84**, 6086 (2000).
[19] G.-M. Zhao, D. J. Kang, W. Prellier, M. Rajeswari, H. Keller, T. Venkatesan, and R. L. Greene, Phys. Rev. B **63**, 060402 (2000).
[20] X. J. Chen, H.-U. Habermeier, C. L. Zhang, H. Zhang, and C. C. Almasan, Phys. Rev. B **67**, 134405 (2003).
[21] P. Schiffer, A. P. Ramirez, W. Bao, and S.-W. Cheong, Phys. Rev. Lett. **75**, 3336 (1995).
[22] X. Wang and X.-G. Zhang, Phys. Rev. Lett. **82**, 4276 (1999).
[23] J. Burgy, M. Mayr, V. Martin-Mayor, A. Moreo, and E. Dagotto, Phys. Rev. Lett. **87**, 277202 (2001).
[24] D. Akahoshi, M. Uchida, Y. Tomioka, T. Arima, Y. Matsui, and Y. Tokura, Phys. Rev. Lett. **90**, 177203 (2003).
[25] Y. Motome, N. Furukawa, and N. Nagaosa, Phys. Rev. Lett. **91**, 167204 (2003).
[26] V. N. Smolyaninova, X. C. Xie, F. C. Zhang, M. Rajeswari, R. L. Greene, and S. Das Sarma, Phys. Rev. B **62**, 3010 (2000).
[27] A. Tiwari and K. P. Rajeev, Solid State Commun. **111**, 33 (1999).
[28] M. Auslender, A. E. Karkin, E. Rozenberg, and G. Gorodetsky, J. Appl. Phys. **89**, 6639 (2001).
[29] C. L. Zhang, X. J. Chen, C. C. Almasan, J. S. Gardner, and J. L. Sarrao, Phys. Rev. B **65**, 134439 (2002).
[30] D. Kumar, J. Samkar, J. Narayan, R. K. Singh, and A. K. Majumdar, Phys. Rev. B **65**, 094407 (2002).
[31] M. Ziese, Phys. Rev. B **68**, 132411 (2003).
[32] C. A. Perroni, V. Cataudella, G. De Filippis, G. Iadonisi, V. Marigliano Ramaglia, and F. Ventriglia, Phys. Rev. B **68**, 224424 (2003).
[33] M. Angeloni, G. Balestrino, N. Boggio, P. G. Medaglia, P. Orgiani, and A. Tebano, J. Appl. Phys. **96**, 6387 (2004).
[34] A. Yu. Petrov, C. Aruta, S. Mercone, C. Adamo, I. Alessandri, and L. Maritato, Eur. Phys. J. B **40**, 11 (2004).
[35] U. Scotti di Uccio, A. Oropallo, P. Perna, and F. Miletto, (unpublished).
[36] L. J. van der Pauw, Philips Tech. Rev. **20**, 220 (1958).

[37] A. Gupta and J. Z. Sun, J. Magn. Magn. Mater. **200**, 24 (1999); A. Gupta, G. Q. Gong, Gang Xiao, P. R. Duncombe, P. Lecouer, P. Trouilloud, Y. Y. Wang, V. P. Dravid, and J. Z. Sun, Phys. Rev. B **54**, R15 629 (1996) and references therein.
[38] L. Sheng, D. Y. Xing, D. N. Sheng, and C. S. Ting, Phys. Rev. B **56**, R7053 (1997).
[39] N. Furukawa, Y. Shimomura, T. Akimoto, and Y. Morimoto, J. Magn. Magn. Mater. **226**, 782 (2001).
[40] S. Kumar and P. Majumdar, cond-mat/0406084 (unpublished).
[41] C. A. Perroni, G. De Filippis, V. Cataudella, and G. Iadonisi, Phys. Rev. B **64**, 144302 (2001).
[42] J. M. D. Coey, M. Viret, and L. Ranno, Phys. Rev. Lett. **75**, 3910 (1995).
[43] C. P. Adams, J. W. Lynn, Y. M. Mukovskii, A. A. Arsenov, and D. A. Shulyatev, Phys. Rev. Lett. **85**, 3954 (2000).
[44] D. C. Worledge, L. Mieville, and T. H. Geballe, Phys. Rev. B **57**, 15 267 (2003).
[45] N. Mannella, A. Rosenhahn, C. H. Booth, S. Marchesini, B. S. Mun, S.-H. Yang, K. Ibrahim, Y. Tomioka, and C. S. Fadley, Phys. Rev. Lett. **92**, 166401 (2004).
[46] S. Kumar and P. Majumdar, cond-mat/0406085 (unpublished).
[47] Ch. Hartinger, F. Mayr, A. Loidl, and T. Kopp, cond-mat/0404023 (unpublished).
[48] C. Sen, G. Alvarez, and E. Dagotto, Phys. Rev. B **70**, 064428 (2004).